Interfacial adsorption and activity of pancreatic lipase-related protein 2 onto heterogeneous plant lipid model membrane

Jeanne Kergomard, Frédéric Carrière, Gilles Paboeuf, Lauriane Chonchon, Nathalie Barouh, Véronique Vié, Claire Bourlieu-Lacanal

Title: Interfacial adsorption and activity of pancreatic lipase-related protein 2 onto heterogeneous plant lipid model membrane

Name(s) of Author(s) Jeanne Kergomard[1,2], Frédéric Carrière[3], Gilles Paboeuf[1,4], Lauriane Chonchon[1], Nathalie Barouh[5,6], Véronique Vié[1,4*] & Claire Bourlieu[2**]

Author Affiliation(s) [1]IPR Institute of Physics, Rennes 1 University, France; [2]INRAE/UM/Institut Agro Montpellier UMR 1208 IATE, France; [3]Aix-Marseille Université, CNRS, UMR7281 Bioénergétique et Ingénierie des Protéines, Marseille, France ; [4]Univ Rennes, CNRS, ScanMAT - UMS 2001, F-35042, Rennes, France ; [5]CIRAD, UMR QUALISUD, F34398 Montpellier-France, [6]Qualisud, Univ Montpellier, Avignon Université, CIRAD, Institut Agro, Université de La Réunion, Montpellier, France.

C**orresponding authors:**

***Dr. Véronique Vié, Institut de Physique de Rennes, Campus de Beaulieu, UMR UR1 CNRS 6251, Université de Rennes, 35042 Rennes cedex,** phone number: 33 (0)2 23 23 56 45 and E-mail address : veronique.vie@univ-rennes.fr;

****Dr. C. Bourlieu-Lacanal, UMR 1208 IATE, 2 Place Pierre Viala, Bât. 31, INRAE/UM/Institut Agro Montpellier, F34060 MONTPELLIER CEDEX 1**, France, phone number: 33 (0)4 99 61 22 03 and E-mail address : claire.bourlieu-lacanal@inrae.fr

Word count: 7018

Total number of tables/figures: 9

Abbreviations

DGDG: digalactosyldiacylglycerol

DGG: digalactosylglycerol

DGMG: digalactosylmonoacylglycerol

DLS: dynamic light scattering

FFA: free fatty acids

GL: galactolipids (model system)

gPLRP2: guinea pig protein lipase related-protein 2

hPLRP2: human protein lipase related-protein 2

MGDG: monogalactosyldiacylglycerol

MGG: monogalactosylglycerol

MGMG: monogalactosylmonoacylglycerol

PL: phospholipids

PLRP2: protein lipase related-protein 2

PUFA: polyunsaturated fatty acids

pS: phytosterols

ABSTRACT

Pancreatic lipase related-protein 2 (PLRP2) exhibits remarkable galactolipase and phospholipase A1 activities, which depend greatly on the supramolecular organization of the substrates and the presence of surfactant molecules such as bile salts. The objective of the study was to understand the modulation of the adsorption mechanisms and enzymatic activity of Guinea pig PLRP2 (gPLRP2), by the physical environment of the enzyme and the physical state of its substrate. Langmuir monolayers were used to reproduce homogeneous and heterogeneous photosynthetic model membranes containing galactolipids (GL), and/or phospholipids (PL), and/or phytosterols (pS), presenting uncharged or charged interfaces. The same lipid mixtures were also used to form micrometric liposomes, and their gPLRP2 catalyzed digestion kinetics were investigated in presence or in absence of bile salts (NaTDC) during static *in vitro*, so called "bulk", digestion.

The enzymatic activity of gPLRP2 onto the galactolipid-based monolayers was characterized with an optimum activity at 15 mN/m, in the absence of bile salts. gPLRP2 showed enhanced adsorption onto biomimetic model monolayer containing negatively charged lipids. However, the compositional complexity in the heterogeneous uncharged model systems induced a lag phase before the initiation of lipolysis. In bulk, no enzymatic activity could be demonstrated on GL-based liposomes in the absence of bile salts, probably due to the high lateral pressure of the lipid bilayers. In the presence of NaTDC (4 mM), however, gPLRP2 showed both high galactolipase and moderate phospholipase A1 activities on liposomes, probably due to a decrease in packing and lateral pressure upon NaTDC adsorption, and subsequent disruption of liposomes.

KEYWORDS: pancreatic lipase related-protein 2, heterogeneous monolayers, galactolipids, monolayer, liposomes

1 INTRODUCTION

Galactolipids (GL) are the main lipids found in the photosynthetic membrane of plants and algae, accounting for more than 70% wt. of the total membrane lipids (Dörmann, 2013; Douce et al., 1973; Gurevich et al., 1997). Due to the natural abundance of plants and algae on Earth, GL represent the most important class of lipids, and therefore, the most important reservoir of fatty acids (80% versus 20% wt. for plant phospholipids (PL) and TAG), including some essential polyunsaturated fatty acids (PUFA) (Gounaris & Barber, 1983). The two main GL composing the photosynthetic membranes of plants are the neutral monogalactosyldiacylglycerol (MGDG, 53% wt.) and digalactosyldiacylglycerol (DGDG, 27% wt.). MGDG possess a unique small 1-β-galactose polar head bound at the *sn-3* position to a diacylglycerol (Lee, 2000), whereas DGDG has a larger polar head with an additional α-galactose, linked to β-galactose (Mizusawa & Wada, 2012). Both galactolipids possess two esterified acyl chains of fatty acids at the *sn*-1 and *sn*-2 position of the glycerol backbone, whose nature depends mainly on the synthesis pathway of GL (Glöckner, 2013; Sahaka et al., 2020). In addition to these two glycolipids, photosynthetic plant membranes contain smaller amounts of charged lipids, sulfoquinovosyldiacylglycerol (SQDG) and phosphatidylglycerol (PG), the proportions of which vary between photosynthetic plant species. GL are naturally rich in the essential α-linolenic acid (ALA, C18:3 ω3), which is the precursor of longer chain ω3 fatty acids, the eicosapentaenoic acid (EPA, C20:5, ω3), and the docosahexaenoic acid (DHA, C22:6 ω3), resulting from elongation and desaturation reactions (Kergomard et al., 2021). In particular, these two long-chain PUFA play a crucial role in the homeostatic regulation of the human body by being the precursors of signaling oxygenated lipids involved in inflammation resolution processes in our body (Saini & Keum, 2018). GL also contain a significant amount of hexadecatrienoic acid (HTA, C16:3 ω3), an unusual fatty acid found mainly in green plants and

algae. The nutritional benefits of HTA have been scarcely studied, although it represents a unique biomarker of the digestion, absorption, and accretion of GL FA. Indeed, it has been found in tissues of zebrafish fed with chloroplast-rich fractions (Gedi et al., 2019), as well as in the meat of horses (Belaunzaran et al., 2018), and has been identified as a potential precursor of ALA in rodents (Cunnane et al., 1995). The interesting nutritional profile of GL makes them compounds of interest for the development of food products rich in ω3 PUFA. Nevertheless, in order to exploit the nutritional properties of GL in potential food applications, it is necessary to determine their digestibility by humans.

Regarding this digestibility, human pancreatic juice and duodenal contents have been shown to exhibit galactolipase activity (Andersson et al., 1995). This activity was associated to PLRP2 (Andersson et al., 1996), as well as, to a lesser extent, to the bile salt-simulated lipase/carboxyl ester hydrolase (BSSL/CEH) (Amara et al., 2013; Bakala N'Goma et al., 2012). PLRP2 shows enzymatic activity on polar lipid substrates with larger heads in comparison with other classical pancreatic lipases such as HPL. Indeed, in addition to lower lipase activity (1250 *versus* 8500 U/mg for HPL on tributyrin), PLRP2 exhibits some phospholipase A1 (74 U/mg on purified L-α-PC) and high galactolipase (~2800 U/mg on MGDG for instance) activities (Amara et al., 2009; De Caro et al., 2004; Sahaka et al., 2020; Wattanakul et al., 2019). This enzymatic activity on a wider range of substrates than HPL is partly explained by the unusual conformation of the lid controlling the access to the active site of hPLRP2 (Eydoux et al., 2008). PLRP2 is also present in the digestive system of other species, and in particular in monogastric herbivores such as the guinea pig (gPLRP2), whose diet contains significant amounts of GL. Although the galactolipase activity of PLRP2 has been the subject of numerous studies, they were mainly focused on the identification and quantification of enzyme activity on synthetic (medium chain acyl GL) or natural substrates

most of the time presented in the form of micelles with bile salts. In these studies, little attention was given to the local physical state, whether regarding the level of condensation, nor the presence of charged molecules. PLRP2 was also found to be active on monolayers of pure PL and GL, with an optimum activity at surface pressures below the lateral surface pressure of membranes, *i.e.* 10-15 mN/m (Eydoux, De Caro, et al., 2007; Hjorth et al., 1993; Sias et al., 2004). These findings, together with the absence of interaction and activity of PLRP2 on PL liposomes (Mateos-Diaz, Bakala N'Goma, et al., 2018), suggest that PLRP2 may not be able to act directly on plant membranes. In the present study, gPLRP2, whose biochemical properties are close to those of hPLRP2, was used as a model of PLRP2. We proposed to investigate the adsorption mechanisms of PLRP2 on plant model and natural monolayers presenting homogeneous or heterogeneous physical states at the air/water interface, as well as on GL liposomes in static dispersed condition, hereafter called "bulk", in the absence and presence of bile salts (NaTDC, 4 mM). Indeed, bile salts are biosurfactants that are secreted by the liver, and which play key contrasting roles in lipid digestion: they adsorb onto interfaces where they can compete with lipases and inhibit lipolysis (Bezzine et al., 1999; Borgström, 1975), but they also remove lipolysis products from the interface, solubilizing them into micelles (Pabois et al., 2021). More importantly, they form mixed micelles with polar lipids, *i.e.* PL and GL, that are the preferred substrates for pancreatic phospholipase A2 (Borgström, 1993) and PLRP2 (Amara et al., 2010; Mateos-Diaz, Bakala N'Goma, et al., 2018), respectively.

We studied the organizational properties and enzymatic activity of gPLRP2 on different GL substrates, controlling finely their physical state, *i.e.* on systems with or without phase heterogeneities. The adsorption and enzymatic hydrolysis capacity of gPLRP2 were first tested on homogeneous and heterogeneous monolayers of GL, PL, and pS (GL and GL/DPPC/pS

monolayers), as well as on more biomimetic system (MGDG/DGDG/SQDG/PG monolayer), in order to gain a mechanistic understanding of the digestion mechanisms at the lipid interface molecular level (nm). These three lipid mixtures were then formulated into liposomes and incubated in the presence of gPLRP2 to determine if galactolipase and/or phospholipase A1 activities were displayed on these dispersed micronic objects (µm) either in the absence or presence of bile salts (NaTDC).

2 EXPERIMENTAL SECTION

Chloroform, methanol, SQDG, and PG were purchased from Sigma Aldrich Ltd. (St. Louis, MO). *1,2*-dipalmitoylphosphatidylcholine (DPPC), MGDG and DGDG were purchased from Avanti Polar Lipids. Canola pS, composed of a mixture of β-sitosterol (50 mol%), campesterol (40 mol%) and brassicasterol (10 mol%), were kindly donated by Cognis France (Estarac, France). pS were collected from desodorization distillates of canola oil. If not stated otherwise, all biophysical characterizations were conducted at least in triplicate.

2.1 Preparation of lipid mixtures

Binary mixture of natural long chains MGDG and DGDG (60:40, mol/mol) was prepared, namely (1) GL. Heterogeneous mixture of GL, DPPC and pS, namely (2) GL/DPPC/pS (45:45:10, mol/mol/mol), respectively was also prepared both to simplify the composition of natural plant membrane, and to provide a pronounced phase coexistence. A biomimetic model system was also prepared, reproducing more accurately the composition of plant photosynthetic membranes, by the addition of charged polar lipids, SQDG (predominant species C18:3/C16:0) and PG, and hereafter called (3) MGDG/DGDG/SQDG/PG (56:24:10:10, mol/mol/mol/mol). Relative compositions of the model systems and fatty acid repartitions of MGDG and DGDG used in this study are given in Table S1 and Figure S2, respectively.

2.2 Enzyme purification and preparation of aliquots

Recombinant guinea pig pancreatic lipase-related protein 2 (gPLRP2) and its inactive variant gPLRP2 S125G were produced in *Aspergillus orizae* and *Pichia pastoris*, respectively, and purified as described in Hjorth et al. (1993) and Mateos-Diaz et al. (2018). For the interfacial measurements, a gPLRP2 stock solution (0.15 mg/mL) was prepared in a Tris HCl buffer (10 mM Tris, 100 mM

NaCl, 5 mM $CaCl_2$, pH 7) and aliquots were prepared in the same buffer at a final concentration of 0.128 mg/L (2.7 nM). This value is closed to the physiological concentrations divided by 100 and corresponds to the usual value used in interfacial studies to avoid saturating the interface with digestive proteins. The inactive gPLRP2 S125G variant was used as a control of the protein effect on lipids in the absence of any enzyme activity as previously shown with phospholipids (Mateos-Diaz et al., 2018). For digestion experiments in static conditions, 100 µL aliquots were prepared at a final concentration of 3.3 mg/L.

2.3 Ellipsometry and surface pressure measurements at the air/water interface

Kinetic measurements were performed over 2 hours using a computer controlled and user-programmable LB Teflon Langmuir trough (KSV Nima, Helsinki, Finland) with a surface area of 35 cm^2 controlled by two mobile barriers. The Teflon trough has been carefully cleaned with UP water and ethanol before each experiment, and ellipsometric and tensiometric measurements were performed during half an hour on pH 7 buffer to check the cleaned surface.

The surface pressure (π) was measured every 4s with a precision of ± 0.2 mN/m using a filter paper connected to a microelectronic feedback system (Nima Technology, UK), according to the Wilhelmy-plate method. The ellipsometric angle (Δ) was recorded simultaneously every 4 s with a precision of ± 0.5°, using a home-made automated ellipsometer in a "null ellipsometer" configuration (Berge & Renault, 1993; Bourlieu et al., 2020). The laser beam probed a surface of 1 mm^2 and a depth in the order of 1 µm and provided insight on the thickness of the interfacial film formed at the interface.

2.4 Monitoring of the gPLRP2 adsorption onto mixed galactolipid monolayers at the air/water interface

The three monolayers studied were formed by spreading a few microliters of 1 mM solution of lipids in $CHCl_3$/MeOH (2:1, v/v) over the surface of the buffer solution until an initial pressure of 20 ± 1 mN/m (Bénarouche et al., 2013).

After stabilization of the film over 5 minutes, 14.6 µL of gPLRP2 solution (0.15 mg/mL) was diluted with 30 µL Tris buffer and injected in the sub-phase to achieve a final gPLRP2 concentration of 2.7 nM. The evolution of the surface pressure and ellipsometric angle due to the enzyme adsorption and lipolytic activity onto the lipid monolayer was continuously monitored over 45 minutes to 2 hours depending on the system studied, until a final surface pressure of 6 mN/m was reached, this value being the one of the gel-fluid phase transition of DPPC (Xu & Zuo, 2018).

2.5 Analysis of the digestion products present at the interface and in the sub-phase

The interface of the GL monolayer was collected after 1h digestion kinetic, using a home-made vacuum extraction pump system. Lipids were extracted by Folch method before being analyzed by thin layer chromatography (TLC) to determine the concentrations of lipolysis products. The organic phase resulting from the extraction was separated and eluted on TLC plates using a mixture of chloroform/methanol/water (95:20:2.5, v/v/v). The TLC plate revelation was made by dipping the plate in a 50:50 v/v mixture of saturated copper acetate solution in water and 85.5% phosphoric acid solution and subsequent oven drying (180°C, 10min). Revealed bands were then scanned by densitometry (500 nm, TLC Scanner 4, CAMAG) and quantified using VisionCat software.

2.6 Visualization of lipase distribution in heterogeneous film by atomic force microscopy

For AFM imaging, interfacial films were transferred onto a freshly-cleaved mica plate using the Langmuir-Blodgett method at the end of the kinetics, at a constant surface pressure and at a very low speed (0.5 mm/min). For each monolayer, two sampling were performed at different times, in

order to observe the organization of the interface at different stages of lipase adsorption and lipolysis. For the GL monolayer, sampling was performed at 35 minutes and 1 hour, respectively. For the GL/DPPC monolayer, sampling was carried out at 45 minutes and 1 hour and 15 minutes, respectively. For the GL/DPPC/pS monolayer, sampling was done at 45 minutes and 1 hour 45 minutes, respectively. Finally, for the MGDG/DGDG/SQDG/PG, sampling was carried out after 1 hour kinetic. AFM (Multimode Nanoscope 8, Bruker, France) was used for imaging in contact mode QNM in air (20°C), using a standard silicon cantilevers (0.06 N/m, SNL-10, Bruker, France), and at a scan rate of 1 Hz. The force was minimized during all scans and the scanner size was 100×100 μm². The processed images analyzed by the open-source platform Gwyddion were representative of at least duplicated experiments.

2.7 Static digestion of liposomes made from mixed GL, GL/DPPS/pS, and MGDG/DGDG/SQDG/pS systems by gPLRP2

1 μm extruded liposomes of i) GL, ii) GL/DPPC/pS, and iii) MGDG/DGDG/SQDG/PG model solutions, respectively, were prepared at a final concentration of 0.4% wt. in Tris HCl buffer (10 mM Tris, 100 mM NaCl, 5 mM $CaCl_2$, pH 7).

2.6.1 Size distribution of liposomes by dynamic light scattering

The size (diameter, nm) distribution of liposomes was assessed by dynamic light scattering (DLS) with a Malvern Panalytical Zetasizer PRO (Malvern, Worcestershire, United Kingdom) fitted with a 633-nm He-Ne laser at 25 °C. ZS Explorer Software version 3.1.0. (Malvern) was used to collect and analyze the data. Measurement were conducted on 1 mL of liposomes dispersion (after 10 times dilution in mQ water) with equilibration time of 120 s, 10 runs of 120 s measurements were performed with a refractive index of 1.45 for liposomes, respectively. The

intensity, diameter distribution, the hydrodynamic diameter as Z-average, and the polydispersity index (PdI) were deduced from the autocorrelation fit of the data.

2.6.2 Static bulk digestion of liposomes by gPLRP2 in absence and in presence of 4 mM NaTDC

Liposomes were incubated under constant agitation in Tris HCl buffer (10 mM Tris, 100 mM NaCl, 5 mM $CaCl_2$, pH 7) containing gPLRP2 at 3.3 mg/L in absence or in presence of 4 mM NaTDC (above CMC value). 100 µL aliquots were sampled at T_0 (control) and after 5 min of gPLRP2 digestion (T_{5min}), and lipids were extracted by Folch method before being analyzed by thin layer chromatography (TLC) to determine the concentrations of residual substrates and lipolysis products. The organic phase resulting from the extraction was separated and eluted on TLC plates as detailed in section 2.5 above. It was thus possible to monitor the enzymatic activity of gPLRP2 on liposomes of both galactolipid mixtures in absence or presence of bile salt-related detergent (NaTDC, 4 mM).

3 RESULTS AND DISCUSSION

3.1. Interfacial behavior of model lipid monolayers

Lipid-lipid interactions and molecular organization at the air/water interface were investigated at 20 mN/m and pH 7 and are presented in Figure 1. We were able to form stable GL based-monolayers at the air/water interface. The GL interface was characterized by a fluid phase, presenting some roughness due to the intercalation of the polar heads of MGDG and DGDG (Figure 1.A). The GL/DPPC/pS system showed a coexistence of condensed liquid/expanded liquid phases, with the presence of condensed phase domains visible on the AFM images, enriched in DPPC-MGDG and pS (Figure 1.B). Additionally, the presence of pS in condensed domains have induced the appearance of defects, that could modulate the subsequent adsorption of lipolytic enzymes (Bourlieu et al., 2016; Kergomard, Carrière, Paboeuf, Artzner, et al., 2022). For the MGDG/DGDG/SQDG/PG biomimetic monolayer (Figure 1.C), small flower-shaped nanodomains of 1.6 ± 0.1 nm height were evidenced at the air/water interface, coexisting with a fluid phase.

3.2. Interfacial adsorption and enzymatic activity of gPLRP2 onto homogeneous galactolipid monolayer (GL)

The interfacial adsorption and enzymatic activity of gPLRP2 onto homogeneous GL monolayer GL was monitored using tensiometry coupled with ellipsometric measurements. Figure 2.A shows the evolution of surface pressure and ellipsometric angle over one hour after the injection of gPLRP2 at 0.128 mg/L in the subphase. Right after the injection of the enzyme below the GL monolayer, the surface pressure started to decrease drastically, reporting the modifications of the interactions between molecules at the interface and the probable lipolysis of the acyl chains of galactolipids by gPLRP2. When considering the maximal slope of this decreasing curve, it

coincided with a range of surface pressure from 15 to 10 mN/m, *i.e.* a surface pressure where the enzymatic activity of gPLRP2 was the highest. This assumption was consistent with the evolution of the ellipsometric angle, as a sharp drop of $\delta\Delta$=0.8 was obtained at π=15 mN/m (Figure 2.A). Since the activity of gPLRP2 on medium chain MGDG and DGDG monolayer was previously reported to be maximum between 10 to 15 mN/m (De Caro et al., 2004; Eydoux, De Caro, et al., 2007), it is hypothesized that the changes occurring at the interface (π and Δ) results from gPLRP2 activity on the GL monolayer. Given the fact that the surface pressure did not show a significant increase after gPLRP2 injection, contrary to what had been previously observed with other lipases onto heterogeneous monolayers (Bourlieu et al., 2016), it is hypothesized that most gPLRP2 molecules are found right below the surface and do not penetrate into the monolayer. This assumption was consistent with the ellipsometric angle data: no evolution was observed during the first 0.6 hour of kinetic after the lipase injection in the subphase. These data suggest that gPLRP2 adsorption below the surface is quite discrete and limited in comparison to gastric lipase for instance (Bourlieu et al., 2016).

In order to understand the partitioning of the enzyme and the disorganization of the interface induced by the enzymatic activity, two Langmuir-Blodgett sampling of the interface were realized; before and after the drop of the ellipsometric angle. The 5×5 µm² AFM images of the two samples, after 35 min and 1 hour kinetic, respectively, are presented in Figure 2.B. After 35 min of enzymatic kinetic, small flower-like condensed phase domains of 1.9 ± 0.1 nm height appeared at the air/water interface, presumably attributed to the generation of digestion products by the degradation of MGDG and DGDG by gPLRP2, in agreement with the subsequent decrease of the surface pressure. Protuberances of 3.6 ± 0.3 nm height were also visible, very likely being attributed to some lipase molecules adsorbed at the interface. Indeed, such height differences had previously been shown in

the literature to be associated with the presence of self-organized proteins at the interface of a lipid monolayer (Kergomard, Carrière, Paboeuf, Barouh, et al., 2022; Sarkis & Vié, 2020). After 1 hour kinetic, the resulting interface had evolved further. Surprisingly, gPLRP2 seems to have formed a protein network of 3.4 ± 0.1 nm in height, in addition to the protuberances observed on the 35 min images, despite the absence of increase in the surface pressure. Additionally, condensed phase domains have grown, reinforcing the hypothesis of their attribution to the generation of lipolysis products.

Indeed, gPLRP2 is known to hydrolyze the *sn*-1 position of GL, according to the reaction scheme proposed in Figure 3, generating monogalactosylmonoacylglycerol (MGMG) and digalactosylmonoacylglycerol (DGMG) in the case of MGDG and DGDG, respectively, as well as free fatty acids (FFA) (Amara et al., 2010; Withers-Martinez et al., 1996). Due to their polyunsaturated content, it is likely that MGMG and DGMG molecules remained in the fluid phase at the air/water interface, and that the condensed phase domains were probably enriched in saturated fatty acids released by PLRP2. Further hydrolysis of MGMG and DGMG by gPLRP2 can also lead to the production of water-soluble galactosylated products: monogalactosylglycerol (MGG) and digalactosylglycerol (DGG) (Figure 3) (Sahaka et al., 2021). The generation of MGG and DGG could explain the decrease in surface pressure after gPLRP2 injection, as well as the drop in the ellipsometric angle corresponding to a loss of matter at the air/water interface. Additionally, the reorganization of these lipolysis products at the interface and in the aqueous subphase may have resulted in the formation of structural defects, thereby promoting lipolysis. To support the hypothesis of a galactolipid degradation by gPLRP2, leading to the generation of digestion products, the interface and subphase were collected after 1h of kinetics, and the lipid products were analyzed by TLC. The results (supplementary data, Figure S3) indicated the presence of digestion

products (FFA) at the interface and in the subphase, confirming the galactolipase activity of gPLRP2 on the GL model monolayer.

To check which part of the evolution of the surface pressure and the ellipsometric angle was resulting either from the galactolipase activity of gPLRP2, or from the interactions of the protein with the lipid monolayer, the experiment was reproduced using an inactive variant (S125G) of gPLRP2. In this variant, the catalytic serine S152 was replaced by a glycine, resulting in the loss of the enzymatic activity. The S125G variant of gPLRP2 has been previously characterized using Fourier transform infrared spectroscopy (FTIR) in the study of Mateos-Diaz et al. (2018), showing that the inactive variant retained his correct folding compared to active gPLRP2, and that its interfacial behavior should not be affected.

Figure 4.A. presents the kinetic evolution of the surface pressure and ellipsometric angle over 1 hour after the injection of the inactive variant of gPLRP2 into the subphase of the GL monolayer. After the S125G gPLRP2 injection in the subphase, there was no evolution in the surface pressure, nor in the ellipsometric angle, confirming that the variations previously observed with gPLRP2 (Figure 2.A) were due to enzymatic activity. Additionally, AFM image Figure 4.B showed the presence of the same protuberances observed with the active enzyme, with similar height of 3.8 ± 0.2 nm. Thus, it seems that, despite the lack of surface pressure increase, the enzyme gets adsorbed at the interface.

3.3. Modulation of the gPLRP2 adsorption and kinetic activity onto heterogeneous model monolayer of galactolipids, phospholipids and phytosterols (GL/DPPC/pS)

Figure 5.A shows the kinetic evolution of the surface pressure and ellipsometric angle after the injection of gPLRP2 below the GL/DPPC/pS monolayer. A decrease with time in the surface

pressure similar to what was observed with the GL monolayer (Figure 2.A), was observed right after the injection of the enzyme in the subphase. However, the decrease in surface pressure was slower than with the GL monolayer. A drop in the ellipsometric angle ($\delta\Delta$=0.9°) was also observed when the surface pressure reached 15 mN/m, but it occurred at 1.4 h instead of 0.6 h (35 min) with the GL monolayer, reflecting the slowing down of the lipolysis rate. As previously, we assumed that these variations correspond to a loss of matter at the interface, upon lipolysis of the monolayer by gPLRP2 and to the generation of water-soluble MGG and DGG. The lag phase of about 50 min observed with the GL/DPPC/pS monolayer before the initiation of lipolysis could be explained by the higher packing of the heterogeneous monolayer induced by DPPC and pS, and a greater difficulty for gPLRP2 to reach the acyl chains of hydrolysable substrates (galactolipids and DPPC). The previous characterization study of homogeneous and heterogeneous GL monolayers has indeed shown that the addition of DPPC and pS to a GL monolayer led to the formation of condensed phase domains enriched in DPPC and MGDG, reducing the lateral distance between the acyl chains available for gPLRP2 to insert (Kergomard, Carrière, Paboeuf, Artzner, et al., 2022). This higher packing could thus explain the lag phase observed before the gPLRP2 could reach its optimum activity, a high packing density at the air/water interface having been proposed to explain the long induction times observed for other lipases onto tightly packed short-chained phospholipids (Verger et al., 1973) and diacylglycerols (Wieloch et al., 1982) monolayers. The initiation of lipolysis of the GL/DPPC/pS led however to the formation of lipolysis products and to the subsequent decrease in surface pressure and lipid packing, that accelerate the activity of gPLRP2.

Two Langmuir-Blodgett transfers of the monolayer were taken after 45 minutes and 1h45 of kinetics, respectively, and AFM images of the interfacial organization were recorded (Figure 5.B). After 45 minutes of kinetics, condensed domains of 1.5 ± 0.2 nm in height were visible at the

air/water interface. Given the low drop in surface pressure observed at 45 min, these domains are probably not related to the generation of digestion products. Furthermore, the interfacial organization and heights observed were similar to those obtained at T_0 before the injection of gPLRP2 into the subphase (Figure 1.B), supporting the hypothesis that lipolysis is probably not yet initiated at this stage of the kinetics. At 1h45 minutes of kinetics, the surface pressure had reached π=6.3 mN/m, and AFM images of the film interface revealed a very different interfacial organization, consistent with the evolution of surface pressure and the drop in the ellipsometric angle. Thin and discontinuous lines of h_1=3.1 ± 0.2 nm in height were visible in the fluid phase and around the condensed domains, that could correspond to gPLRP2 molecules adsorbed at the monolayer interface. Condensed domains of three different heights were also identified. First, small flower-like shaped condensed domains were visible in the fluid phase, with a height h_2 of 2.0 ± 0.1 nm, probably attributed to the generation of lipolysis product MGMG and DGMG, as observed for the GL monolayer. Fragmented condensed phase domains were also revealed, composed of at least three different height levels (h3, h4, fluid bottom). This observed fragmentation could be due to the disorganization caused by the adsorption and enzymatic activity of gPLRP2, but also to the low-pressure value (π=6.3 mN/m), causing phase segregation within the condensed phase domains thought to be enriched in DPPC-MGDG-pS. Indeed, the lateral pressure was probably no longer sufficient to ensure the miscibility of DPPC and pS with MGDG, causing phase segregation which could explains the observed height differences.

These observations nevertheless confirm the miscibility of these three compounds and the phase heterogeneity in the condensed phase domains at 20 mN/m , as well as the condensation effect of DPPC and pS on MGDG chains observed in our previous study (Kergomard, Carrière, Paboeuf, Artzner, et al., 2022). Given the molar composition of the GL/DPPC/pS monolayer, the central

rounded domain (h_3=1.7 ± 0.2) observed at 1h45 of kinetic could be attributed to the presence of condensed DPPC. The smaller domains of h_3 and h_4 heights, coexisting with the fluid phase, could be attributed to the presence of FFA and pS, coexisting with MGDG and MGMG in the fluid phase.

In the considered range of surface pressure, it is indeed unlikely that gPLRP2 shows significant enzymatic activity on DPPC, since monolayer studies have shown that gPLRP2 was only active on this substrate at low surface pressure ($\pi < 5$ mN/m) and was totally inactive at $\pi > 10$ mN/m (Hjorth et al., 1993). However, it remains difficult to attribute each type of domain to a species of molecule, given the complex interactions and differences in miscibility observed in this type of ternary mixture. Surface composition studies will be needed to answer these questions, but the small quantities used for interfacial characterizations do not facilitate such analyses.

3.4. Influence of the presence of charged lipids on the adsorption capacity and enzymatic activity of gPLRP2 in model biomimetic lipid monolayer (MGDG/DGDG/SQDG/PG)

The impact of a charged interface on the adsorption capacities and enzymatic activity of gPLRP2 was studied using MGDG/DGDG/SQDG/PG biomimetic model monolayer. The evolution of surface pressure and ellipsometric angle upon the adsorption of gPLRP2 at the air/water interface is presented Figure 6.A. A continuous decrease of the surface pressure was observed right after the injection of gPLRP2 in the sub-phase until it reached a value of π=8.5 mN/m after 1h of kinetic. In contrast to the GL/DPPC/pS complex system, no lag phase was observed before the onset of lipolysis, and the decrease was continuous, revealing a constant enzymatic activity of gPLRP2 over the 1h kinetic. This observation could be explained by the presence of negatively charged lipids at the interface (SQDG, PG), which could facilitate the adsorption of gPLRP2 underneath the monolayer, and the subsequent degradation of galactolipids. The facilitated adsorption onto a charged surface was previously observed for recombinant dog gastric lipase (rDGL) at the level of

heterogeneous monolayers of polar dairy lipids, with the establishment of electrostatic interactions between the interface and the interfacial recognition site facilitating the orientation and approach of the active site onto the lipid substrates (Bourlieu et al., 2016). In our case however the surface potential electrostatic distribution of charge is very different between rDGL and gPLRP2, but seems to result in favorable interactions with negatively charged lipid interface. The ellipsometric angle did not significantly evolved during the first 30 minutes of the kinetics. After this, it decreased again ($\delta\Delta$=-0.7°) at π=15 mN/m, in the range of the optimal surface pressure for the activity of gPLRP2, as previously observed on GL and GL/DPPC/pS monolayers. The ellipsometric angle then slowly decreased until it reached a value of Δ=5.2° after 1h kinetic, reflecting a decrease in the thickness of the monolayer due to the degradation of GL and the progressive release of polar lipolysis products into the subphase.

Langmuir-Blodgett transfer of the interface was performed on the MGDG/DGDG/SQDG/PG monolayer after 1 kinetic. AFM image (Figure 6.B) after 1h kinetic of incubation with gPLRP2 showed the coexistence of LC snowflake-shape domains of 2.2 ± 0.1 in height in the fluid phase. These domains shared a similar morphology with those obtained after 35 minutes of digestion of the GL monolayer by gPLRP2, and can therefore be attributed to the generation of FFA digestion products by galactolipid degradation. As previously observed, small protuberances of 3.3 ± 0.3 nm in height were also observed, attributed to the adsorbed gPLRP2 molecules in the fluid phase.

3.5. Interaction of liposomal structures (GL, GL/DPPC/pS, MGDG/DGDG/SQDG/PG) with bile salts

Since the interfacial characterization of gPLRP2 interaction with mixed galactolipid monolayer revealed some lipolytic activity, we then evaluate the ability of gPLRP2 to interact with liposomes

made with the same lipid mixture, in the presence and absence of bile salts, to mimic the conditions found in the gastrointestinal tract. We first characterized the effects of bile salts on the liposomal dispersions using DLS.

In the absence of bile salts, GL liposomes showed a monomodal distribution centered at 198 nm while GL/DPPC/pS liposomes were much larger with a monomodal distribution centered at 2990 nm (Figure 7), although both objects had been extruded 10 times over filters of 1 µm pore diameter. Upon the addition of NaTDC (4 mM), bimodal distributions appeared with peaks at 894 and 117 nm for GL liposomes and at 2990 and 146 nm for GL/DPPC/pS. The presence of NaTDC had therefore a strong impact on lipid organization with changes in particle size distribution, a major shift towards larger objects but also the appearance of smaller populations. Ultimately, GL and PL mixed with micellar concentrations of bile salts are known to form mixed micelles with diameter of 10 to 40 nm (Mazer et al., 1980). In that case, DLS is not the most appropriate techniques for covering such large variations in particle size distribution. Nevertheless, it allowed showing lipid re-organization upon the addition of bile salts. The size increase observed with the larger objects could be partially explained by a destabilization of the liposomes during the adsorption of NaTDC at the interface, leading to their fusion. Additionally, the adsorption of NaTDC onto liposomes could have resulted in a diminished GL packing, explaining the larger diameter observed. The smallest objects observed could be related to the desorption of some lipid molecules from the bilayer stabilizing the liposomes. Indeed, previous studies had already investigated the interfacial behavior of NaTDC at the level of assembled lipid structures, and have highlighted its desorption capacities. As an example, (Pabois et al., 2019) have studied the adsorption behavior of NaTDC at the air/water interface, and its interaction with a monolayer of phospholipids (DPPC), mimicking the organization of physiological compounds present at the interface of fat droplets. Firstly, the

results showed a very fast adsorption of NaTDC at the air/water interface at low concentration (< 1 mM), forming stable but irregular film, which was attributed to its unusual polar planar structure and large surface area (Maldonado-Valderrama et al., 2011, 2014). However, these bile salt concentrations were below the critical micellar concentration (CMC) (Roda et al., 1983). At higher concentrations (> 5 mM; *i.e.* > CMC), the addition of bile salts was shown to lead to a decrease in thickness, demonstrating that NaTDC partially desorbs from the interface. The interaction of NaTDC with the DPPC was then studied. Results showed the strong desorption of DPPC molecules (to approximately 40%) from the interface upon the NaTDC adsorption, resulting in the formation of domains with distinct organization. Additionally, increasing the amount of NaTDC have been shown to decrease the DPPC monolayer packing. These results illustrate the well-known micellar solubilization effect of bile salts, leading to the formation of mixed micelles in bulk (Hofmann, 1963; Hofmann & Borgström, 1964; Pabois et al., 2021).

In the case of the GL/DPPC/pS liposomes in the absence of bile salts, they showed an average diameter of 2990 nm that was much larger than the average diameter measured in the case of the GL system (198 nm). The fact that their diameter was larger than 1 µm despite the filter used during extrusion indicates that these objects were relatively stable, as they were able to deform during extrusion without breaking. The appearance of a population of smaller objects upon addition of NaTDC could reflect the re-organization induced by NaTDC molecules. Nevertheless, it seems that the GL/DPPC/pS system remains stable even in the presence of bile salts, as the population of larger droplets remained similar in size in the absence and presence of bile salts

3.6. Interaction of gPLRP2 with galactolipid-based liposomes in the absence and presence of bile salts

As the adsorption capacities and enzymatic activity of gPLRP2 is highly dependent on the substrate organization (Mateos-Diaz, Bakala N'Goma, et al., 2018; Mateos-Diaz, Sutto-Ortiz, et al., 2018), the changes observed with liposomes following the addition of bile salts could most likely modify the access of the enzyme to its substrate and its lipolytic activity.

The impact of bile salt on the galactolipase and phospholipase A1 activities of gPLRP2 was thus assayed in "bulk conditions" using GL/DPPC/pS dispersed liposomes, this system having been shown to be the most stable even in presence of bile salts. No significant hydrolysis activity on GL/DPPC/pS liposomes could be detected in the absence of bile salts after 5 minutes of incubation with gPLRP2 (supplementary material, Table S4). This result was in line with the previous study by Mateos-Diaz et al. (2018), which has shown that gPLRP2 did not possess enzymatic activity on DPPC liposomes in absence of bile salts. These results were however in disagreement with the results obtained with monolayers of the same lipid mixture, on which the lipolytic activity of gPLRP2 was detected (see figure 2 presented in section 3.3 - monolayer results). Nevertheless, the surface pressure of the lipid monolayer at the air/water interface was optimum for the adsorption and enzymatic activity of gPLRP2, which may explain the observed lipolysis under these conditions. The organization of lipids into monolayers is indeed different from that of the bilayers surrounding liposomes, and higher lateral pressure and packing of the latter systems could prevent gPLRP2 from penetrating and degrading its substrate (Kergomard, Carrière, Paboeuf, Artzner, et al., 2022).

However, when bile salts were added to GL/DPPC/pS liposomes, a lipolytic activity of gPLRP2 could be detected by TLC analysis of lipolysis products (Table 1). After 5-min incubation, around 74% wt. of MGDG and 55% wt. of DGDG were converted into MGMG and DGMG, respectively, with the production of FFA. Given the differences in the substrate and lipolysis product

concentrations, it is likely that some MGMG and DGMG have been in turn converted into monogalactosylglycerol (MGG) and digalactosylglycerol (DGG), respectively, by gPLRP2 but these two compounds being water-soluble, they could not be extracted and revealed upon TLC analysis of the organic phase (Sahaka, 2020). It should be noted that the quantification of DGMG after 5 minutes digestion was hampered, given the fact that its retention factor was similar to that of DPPC on the TLC plate. The galactolipase activity observed in the presence of bile salts could be due to the adsorption of NaTDC at the liposome interface, decreasing the lateral pressure and interfacial packing of polar lipids, as previously observed with DPPC domains (Pabois et al. 2019), and thus creating more favorable conditions for the adsorption and activity of gPLRP2. Nevertheless, it cannot be excluded that polar lipids from liposomes were gradually solubilized into mixed micelles prior to their hydrolysis by gPLRP2. This latter hypothesis is supported by the preference of gPLRP2 for micellar substrates (Mateos-Diaz, Bakala N'Goma, et al., 2018). Moreover, the difficulty for gPLRP2 to access it substrate in liposomes was confirmed here when GL/DPPC/pS liposomes were tested in the absence of bile salts.

In addition to the galactolipase activity of gPLRP2, the TLC analysis of lipolysis products also revealed the phospholipase activity of gPLRP2 on the DPPC present in GL/DPPC/pS liposomes, in the presence of bile salts. These results confirm the previous study by Mateos-Diaz et al. (2018) which has shown that gPLRP2 was active on mixed bile salts/DPPC micelles, but not on DPPC liposomes in the absence of bile salts. As in the case of galactolipid hydrolysis, two main hypotheses can be raised about the mode of action of gPLRP2 on PL: a decrease in the packing of the bilayer by bile salts that could promote gPLRP2 adsorption and activity, or the conversion of liposomes into micelles containing DPPC.

Given the lack of activity of gPLRP2 on GL-based liposomes in the absence of bile salts, mixed MGDG/DGDG/SQDG/PG liposomes mimicking the lipid composition of thylakoid membranes were also tested in presence of bile salts. After 5 minutes incubation with gPLRP2 in presence of 4 mM NaTDC (Table 1), about 90% wt. of MGDG and 94% wt. of DGDG were hydrolyzed, while FFA and MGDG were produced. More interestingly, gPLRP2 was also able to hydrolyze 91% of the initial SQDG substrate (Table 1), emphasizing its action on all galactolipids (Andersson et al., 1996). This result confirmed the ability of gPLRP2 to hydrolyze GL from liposomes in the presence of bile salts.

The ability of gPLRP2 to hydrolyze galactolipid membranes even in the absence of bile salts was however recently shown by FTIR on natural chloroplast membranes (Sahaka et al., 2023). This result could be explained by the fact that these natural systems are more complex than the model systems considered in this study, and naturally include negatively charged lipids, shown to enhance the adsorption and extent of lipolysis on model monolayers, independently of the presence of bile salts. Thus, pursuing this study by exploring the degradation of liposomes with more complex compositions in the absence of bile salts, for example MGDG/DGDG/SQDG/PG, could provide insight into the composition at which a galactolipid liposome can become a gPLRP2 substrate.

3.7. Interfacial organization of GL and GL/DPPC/pS liposomes in presence of bile salts obtained at T_0 and after 5 min of gPLRP2 digestion

Lipids products obtained at T_0 and after 5 minutes incubation of GL or GL/DPPC/pS liposomes in the presence of gPLRP2 and bile salts were extracted by Folch method and deposited at the air/water interface at $\pi=7.2 \pm 0.1$ mN/m. We chose to deposit the lipids at this surface pressure in order to approximate the organization of the substrates and digestion products of the interfacial films obtained at the end of the monolayer digestion kinetics for the GL, GL/DPPC/pS, and

MGDG/DGDG/SQDG/PG systems, respectively (π between 5 to 8 mN/m). After stabilization of the respective T_0 and T_{5min} films, Langmuir-Blodgett samples were observed in AFM. For both systems, the images obtained at T_0 and T_{5min} are displayed in Figure 8. For the GL system, AFM images obtained at T_0 revealed the presence of small condensed domains of $h_1=1.3 \pm 0.1$ nm height, that could be attributed to the presence of some NaTDC adsorbed at the air/water interface. At T_{5min}, flower-shape domains of $h_{1'}=1.9 \pm 0.1$ nm in height were evidenced, similar to those obtained after 2h hour kinetic digestion of GL monolayer by gPLRP2 at the air/water interface. These domains were attributed to the generation of the FFA by lipolysis of MGDG and DGDG, in agreement with their detection by TLC (Table 1).

For the GL/DPPC/pS system, the interface obtained at T_0 was clearly different from the one obtained for the GL/DPPC/pS monolayer at 20 mN/m during the interfacial study (section 3.1), but was similar to the one obtained two hours after injecting gPLRP2 in the subphase, when the surface pressure reached π=6.3 mN/m (Figure 2B). Thus, the low surface pressure could explain the fragmentation of the condensed phase domains, as previously observed, with two identified height levels (h1 and h2) probably enriched in DPPC and pS, coexisting with a fluid phase probably enriched in MGDG. Additionally, the inclusion of bile salts at the interface could have spaced out the neighboring DPPC molecules, thus disordering their tight packing and the interfacial organization (Chu et al., 2010). At T_{5min}, the highest domains became more numerous, probably related to the generation of FFA, with a height h1'=1.7 ± 0.1 nm. The organization of the interface was similar to that obtained in the images at 2h kinetics after injection of gPLRP2 in the subphase of GL/DPPC/pS monolayers, highlighting the galactolipase activity of gPLRP2 at the level of heterogeneous liposomes in the presence of bile salts, but also at the level of heterogeneous monolayers.

OVERALL SUMMARY

The adsorption and enzymatic activity of gPLRP2 was studied on GL-based substrates exhibiting different supramolecular structures, and presenting or not phase heterogeneity. The galactolipase activity of gPLRP2 was evidenced at the level of both homogeneous GL and heterogenous GL/DPPC/pS monolayers, after a decrease in surface pressure that allowed reaching the optimum range for gPLRP2 activity on substrate monolayers (Amara et al., 2013; Eydoux, Caro, et al., 2007; Hjorth et al., 1993; Sias et al., 2004). The presence of charged lipids (SQDG, PG) at the interface improved the adsorption capacities of the enzyme through the establishment of electrostatic interactions between the substrate and the interfacial recognition site of the active site, resulting in improved adsorption and enzymatic activity of gPLRP2. The optimal activity of gPLRP2 was obtained at a surface pressure of 15 mN/m for homogeneous or heterogeneous systems, even if the tighter packing of the heterogeneous monolayer has induced a lag phase period before the on-set of the lipolysis.

However, no galactolipase activity could be detected on liposomes made with the same lipid mixtures, confirming the previous finding that gPLRP2 does not interact with phospholipid (DPPC) liposomes and does not display phospholipase A1 on this form of substrate. Therefore, galactolipid-based liposomes are not equivalent to monolayers of the same lipids in terms of recognition by gPLRP2. Since we have shown that gPLRP2 preferentially binds at boundaries between liquid and condensed phases in monolayers, one can assume that lateral packing of lipid molecules and phase heterogeneity are not the same in liposomes. gPLRP2 adsorption to heterogeneous monolayers induces a decrease in surface pressure that further accelerates enzyme activity. This mechanism of action seems to be impaired with liposomes in the absence of bile salts.

Nevertheless, both galactolipase and phospholipase A1 activities of gPLRP2 were detected when heterogeneous GL/DPPC/pS liposomes were incubated in the presence of bile salts. Bile salt adsorption onto the liposomes can accelerate enzyme activity by changing the interfacial properties and this is probably one of the mechanisms by which gPLRP2 becomes active on liposomes. However, knowing the micellar solubilization properties of bile salts on polar lipids and the preference of gPLRP2 for micellar substrates, one can speculate that lipolysis of both GL and PL rapidly proceeds through liposomes disruption and formation of mixed micelles onto which gPLRP2 preferentially binds.

Monolayer studies with heterogeneous lipid films revealed that the presence of surfactants like bile salts is not an absolute requirement to accelerate gPLRP2 activity on GL. It is now tempting to investigate whether gPLRP2 can act directly on plant membranes.

CONCLUSION

The enzymatic activity of gPLRP2 was evidenced onto the galactolipid-based monolayers, with an optimum activity in the range of 10 to 15 mN/m, in the absence of bile salts. The adsorption capacity of gPLRP2 and the subsequent extent of lipolysis, however, was dependent on the chemical composition, but also on the physical environment of the monolayer substrates. In bulk, no enzymatic activity has been evidenced on GL-based liposomes in the absence of bile salts, probably due to the high lateral pressure of the lipid bilayers. In the presence of NaTDC (4 mM), however, gPLRP2 showed both high galactolipase and moderate phospholipase A1 activities on liposomes, probably due to a decrease in packing and lateral pressure upon NaTDC adsorption, and subsequent disruption of liposomes.

601

Declaration of Competing Interest

The authors declare that they have no known competing financial interests or personal relationships that could have appeared to influence the work reported in this paper.

Funding

This research work has been conducted thanks to a research grant from the French Ministry of Research.

Acknowledgments

The authors would like to thank the BIOMIF platform (‘Biological Molecules at fluid interfaces’, IPR, Rennes, France) for allowing the biophysical characterization of samples presented in this article.

C. Bourlieu, V. Vié, F. Carrière, and J. Kergomard determined the outline and the content of the manuscript. J. Kergomard wrote the manuscript and all the authors participated in the experimental design, the collection, the interpretation of data, and the correction and implementation of the manuscript. All authors have approved the final article.

References

Amara, S., Barouh, N., Lecomte, J., Lafont, D., Robert, S., Villeneuve, P., De Caro, A., & Carrière, F. (2010). Lipolysis of natural long chain and synthetic medium chain galactolipids by pancreatic lipase-related protein 2. *Biochimica et Biophysica Acta (BBA) - Molecular and Cell Biology of Lipids*, *1801*(4), 508-516. https://doi.org/10.1016/j.bbalip.2010.01.003

Amara, S., Lafont, D., Fiorentino, B., Boullanger, P., Carrière, F., & De Caro, A. (2009). Continuous measurement of galactolipid hydrolysis by pancreatic lipolytic enzymes using the pH-stat technique and a medium chain monogalactosyl diglyceride as substrate. *Biochimica et Biophysica Acta (BBA) - Molecular and Cell Biology of Lipids*, *1791*(10), 983-990. https://doi.org/10.1016/j.bbalip.2009.05.002

Amara, S., Lafont, D., Parsiegla, G., Point, V., Chabannes, A., Rousset, A., & Carrière, F. (2013). The galactolipase activity of some microbial lipases and pancreatic enzymes. *European Journal of Lipid Science and Technology*, *115*(4), 442-451. https://doi.org/10.1002/ejlt.201300004

Andersson, L., Bratt, C., Arnoldsson, K. C., Herslöf, B., Olsson, N. U., Sternby, B., & Nilsson, A. (1995). Hydrolysis of galactolipids by human pancreatic lipolytic enzymes and duodenal contents. *Journal of Lipid Research*, *36*(6), 1392-1400.

Andersson, L., Carrière, F., Lowe, M. E., Nilsson, Å., & Verger, R. (1996). Pancreatic lipase-related protein 2 but not classical pancreatic lipase hydrolyzes galactolipids. *Biochimica et Biophysica Acta (BBA) - Lipids and Lipid Metabolism*, *1302*(3), 236-240. https://doi.org/10.1016/0005-2760(96)00068-9

Bakala N'Goma, J.-C., Amara, S., Dridi, K., Jannin, V., & Carrière, F. (2012). Understanding the lipid-digestion processes in the GI tract before designing lipid-based drug-delivery systems. *Therapeutic Delivery*, *3*(1), 105-124. https://doi.org/10.4155/tde.11.138

Belaunzaran, X., Lavín, P., Mantecón, A. R., Kramer, J. K. G., & Aldai, N. (2018). Effect of slaughter age and feeding system on the neutral and polar lipid composition of horse meat. *Animal : An International Journal of Animal Bioscience*, *12*(2). https://doi.org/10.1017/S1751731117001689

Bénarouche, A., Point, V., Parsiegla, G., Carrière, F., & Cavalier, J.-F. (2013). New insights into the pH-dependent interfacial adsorption of dog gastric lipase using the monolayer technique. *Colloids and Surfaces B: Biointerfaces*, *111*, 306-312. https://doi.org/10.1016/j.colsurfb.2013.06.025

Berge, B., & Renault, A. (1993). Ellipsometry Study of 2D Crystallization of 1-Alcohol Monolayers at the Water Surface. *Europhysics Letters (EPL)*, *21*(7), 773-777. https://doi.org/10.1209/0295-5075/21/7/010

Bezzine, S., Ferrato, F., Ivanova, M. G., Lopez, V., Verger, R., & Carrière, F. (1999). Human Pancreatic Lipase : Colipase Dependence and Interfacial Binding of Lid Domain Mutants. *Biochemistry*, *38*(17), 5499-5510. https://doi.org/10.1021/bi982601x

Borgström, B. (1975). On the interactions between pancreatic lipase and colipase and the substrate, and the importance of bile salts. *Journal of Lipid Research*, *16*(6), 411-417.

Borgström, B. (1993). Phosphatidylcholine as substrate for human pancreatic phospholipase A2. Importance of the physical state of the substrate. *Lipids*, *28*(5), 371-375. https://doi.org/10.1007/BF02535932

Bourlieu, C., Mahdoueni, W., Paboeuf, G., Gicquel, E., Ménard, O., Pezennec, S., Bouhallab, S., Deglaire, A., Dupont, D., Carrière, F., & Vié, V. (2020). Physico-chemical behaviors of

human and bovine milk membrane extracts and their influence on gastric lipase adsorption. *Biochimie, 169*, 95-105. https://doi.org/10.1016/j.biochi.2019.12.003

Bourlieu, C., Paboeuf, G., Chever, S., Pezennec, S., Cavalier, J.-F., Guyomarc'h, F., Deglaire, A., Bouhallab, S., Dupont, D., Carrière, F., & Vié, V. (2016). Adsorption of gastric lipase onto multicomponent model lipid monolayers with phase separation. *Colloids and Surfaces B: Biointerfaces*, *143*, 97-106. https://doi.org/10.1016/j.colsurfb.2016.03.032

Chu, B.-S., Gunning, A. P., Rich, G. T., Ridout, M. J., Faulks, R. M., Wickham, M. S. J., Morris, V. J., & Wilde, P. J. (2010). Adsorption of Bile Salts and Pancreatic Colipase and Lipase onto Digalactosyldiacylglycerol and Dipalmitoylphosphatidylcholine Monolayers. *Langmuir*, *26*(12), 9782-9793. https://doi.org/10.1021/la1000446

Cunnane, S. C., Hamadeh, M. J., Liede, A. C., Thompson, L. U., Wolever, T. M., & Jenkins, D. J. (1995). Nutritional attributes of traditional flaxseed in healthy young adults. *The American Journal of Clinical Nutrition*, *61*(1), 62-68. https://doi.org/10.1093/ajcn/61.1.62

De Caro, J., Sias, B., Grandval, P., Ferrato, F., Halimi, H., Carrière, F., & De Caro, A. (2004). Characterization of pancreatic lipase-related protein 2 isolated from human pancreatic juice. *Biochimica et Biophysica Acta (BBA) - Proteins and Proteomics, 1701*(1), 89-99. https://doi.org/10.1016/j.bbapap.2004.06.005

Dörmann, P. (2013). Galactolipids in Plant Membranes. In *ELS*. John Wiley & Sons, Ltd. https://doi.org/10.1002/9780470015902.a0020100.pub2

Douce, R., Holtz, R. B., & Benson, A. A. (1973). Isolation and Properties of the Envelope of Spinach Chloroplasts. *Journal of Biological Chemistry*, *248*(20), 7215-7222.

Eydoux, C., Caro, J. D., Ferrato, F., Boullanger, P., Lafont, D., Laugier, R., Carrière, F., & Caro, A. D. (2007). Further biochemical characterization of human pancreatic lipase-related

protein 2 expressed in yeast cells. *Journal of Lipid Research*, *48*(7), 1539-1549. https://doi.org/10.1194/jlr.M600486-JLR200

Eydoux, C., De Caro, J., Ferrato, F., Boullanger, P., Lafont, D., Laugier, R., Carrière, F., & De Caro, A. (2007). Further biochemical characterization of human pancreatic lipase-related protein 2 expressed in yeast cells. *Journal of Lipid Research*, *48*(7), 1539-1549. https://doi.org/10.1194/jlr.M600486-JLR200

Eydoux, C., Spinelli, S., Davis, T. L., Walker, J. R., Seitova, A., Dhe-Paganon, S., De Caro, A., Cambillau, C., & Carrière, F. (2008). Structure of Human Pancreatic Lipase-Related Protein 2 with the Lid in an Open Conformation,. *Biochemistry*, *47*(36), 9553-9564. https://doi.org/10.1021/bi8005576

Gedi, M. A., Magee, K. J., Darwish, R., Eakpetch, P., Young, I., & Gray, D. A. (2019). Impact of the partial replacement of fish meal with a chloroplast rich fraction on the growth and selected nutrient profile of zebrafish (Danio rerio). *Food & Function*, *10*(2), 733-745. https://doi.org/10.1039/C8FO02109K

Glöckner, C. (2013). *The donor and acceptor side of photosystem II : Structural and functional investigations*. https://doi.org/10.14279/depositonce-152

Gurevich, V., Bondarenko, B., Gundermann, K. J., Schumacher, R., Astashkina, T., Ivanov, V., Popov, Y., Shatilina, L., & Kazennova, N. (1997). Poly-unsaturated phospholipids increase the hypolipidemic effect of Lovastatin. *European Journal of Internal Medicine*, *8*(1), 15-20.

Hjorth, A., Carriere, F., Cudrey, C., Woldike, H., Boel, E., Lawson, D. M., Ferrato, F., Cambillau, C., & Dodson, G. G. (1993). A structural domain (the lid) found in pancreatic lipases is absent in the guinea pig (phospho)lipase. *Biochemistry*, *32*(18), 4702-4707. https://doi.org/10.1021/bi00069a003

Hofmann, A. F. (1963). The function of bile salts in fat absorption. The solvent properties of dilute micellar solutions of conjugated bile salts. *Biochemical Journal*, *89*(1), 57-68.

Hofmann, A. F., & Borgström, B. (1964). The Intraluminal Phase of Fat Digestion in Man : The Lipid Content of the Micellar and Oil Phases of Intestinal Content Obtained during Fat Digestion and Absorption*. *Journal of Clinical Investigation*, *43*(2), 247-257.

Kergomard, J., Carrière, F., Barouh, N., Villeneuve, P., Vié, V., & Bourlieu, C. (2021). Digestibility and oxidative stability of plant lipid assemblies : An underexplored source of potentially bioactive surfactants? *Critical Reviews in Food Science and Nutrition*, 1-20. https://doi.org/10.1080/10408398.2021.2005532

Kergomard, J., Carrière, F., Paboeuf, G., Artzner, F., Barouh, N., Bourlieu, C., & Vié, V. (2022). Interfacial organization and phase behavior of mixed galactolipid-DPPC-phytosterol assemblies at the air-water interface and in hydrated mesophases. *Colloids and Surfaces B: Biointerfaces*, 112646. https://doi.org/10.1016/j.colsurfb.2022.112646

Kergomard, J., Carrière, F., Paboeuf, G., Barouh, N., Bourlieu-Lacanal, C., & Vié, V. (2022). Modulation of gastric lipase adsorption onto mixed galactolipid-phospholipid films by addition of phytosterols. *Colloids and Surfaces B: Biointerfaces*, *220*, 112933. https://doi.org/10.1016/j.colsurfb.2022.112933

Lee. (2000). Membrane lipids : It's only a phase. *Current Biology*, *10*(10), R377-R380. https://doi.org/10.1016/S0960-9822(00)00477-2

Maldonado-Valderrama, J., Muros-Cobos, J. L., Holgado-Terriza, J. A., & Cabrerizo-Vílchez, M. A. (2014). Bile salts at the air–water interface : Adsorption and desorption. *Colloids and Surfaces B: Biointerfaces*, *120*, 176-183. https://doi.org/10.1016/j.colsurfb.2014.05.014

Maldonado-Valderrama, J., Wilde, P., Macierzanka, A., & Mackie, A. (2011). The role of bile salts in digestion. *Advances in Colloid and Interface Science*, *165*(1), 36-46. https://doi.org/10.1016/j.cis.2010.12.002

Mateos-Diaz, E., Bakala N'Goma, J.-C., Byrne, D., Robert, S., Carrière, F., & Gaussier, H. (2018). IR spectroscopy analysis of pancreatic lipase-related protein 2 interaction with phospholipids : 1. Discriminative recognition of mixed micelles versus liposomes. *Chemistry and Physics of Lipids*, *211*, 52-65. https://doi.org/10.1016/j.chemphyslip.2017.02.005

Mateos-Diaz, E., Sutto-Ortiz, P., Sahaka, M., Byrne, D., Gaussier, H., & Carrière, F. (2018). IR spectroscopy analysis of pancreatic lipase-related protein 2 interaction with phospholipids : 2. Discriminative recognition of various micellar systems and characterization of PLRP2-DPPC-bile salt complexes. *Chemistry and Physics of Lipids*, *211*, 66-76. https://doi.org/10.1016/j.chemphyslip.2017.11.012

Mazer, N. A., Benedek, G. B., & Carey, M. C. (1980). Quasielastic light-scattering studies of aqueous biliary lipid systems. Mixed micelle formation in bile salt-lecithin solutions. *Biochemistry*, *19*(4), 601-615. https://doi.org/10.1021/bi00545a001

Mizusawa, N., & Wada, H. (2012). The role of lipids in photosystem II. *Biochimica et Biophysica Acta (BBA) - Bioenergetics*, *1817*(1), 194-208. https://doi.org/10.1016/j.bbabio.2011.04.008

Pabois, O., Lorenz, C. D., Harvey, R. D., Grillo, I., Grundy, M. M.-L., Wilde, P. J., Gerelli, Y., & Dreiss, C. A. (2019). Molecular insights into the behaviour of bile salts at interfaces : A key to their role in lipid digestion. *Journal of Colloid and Interface Science*, *556*, 266-277. https://doi.org/10.1016/j.jcis.2019.08.010

Pabois, O., Ziolek, R. M., Lorenz, C. D., Prévost, S., Mahmoudi, N., Skoda, M. W. A., Welbourn, R. J. L., Valero, M., Harvey, R. D., Grundy, M. M.-L., Wilde, P. J., Grillo, I., Gerelli, Y., & Dreiss, C. A. (2021). Morphology of bile salts micelles and mixed micelles with lipolysis products, from scattering techniques and atomistic simulations. *Journal of Colloid and Interface Science*, *587*, 522-537. https://doi.org/10.1016/j.jcis.2020.10.101

Roda, A., Hofmann, A. F., & Mysels, K. J. (1983). The influence of bile salt structure on self-association in aqueous solutions. *The Journal of Biological Chemistry*, *258*(10), 6362-6370.

Sahaka. (2020). *Etude de l'hydrolyse enzymatique des galactolipides par diverses approches chromatographique et spectroscopiques* [These de doctorat, Aix-Marseille]. http://www.theses.fr/2020AIXM0467

Sahaka, M., Amara, S., Lecomte, J., Rodier, J.-D., Lafont, D., Villeneuve, P., Gontero, B., & Carrière, F. (2021). Quantitative monitoring of galactolipid hydrolysis by pancreatic lipase-related protein 2 using thin layer chromatography and thymol-sulfuric acid derivatization. *Journal of Chromatography B*, *1173*, 122674. https://doi.org/10.1016/j.jchromb.2021.122674

Sahaka, M., Amara, S., Wattanakul, J., Gedi, M. A., Aldai, N., Parsiegla, G., Lecomte, J., Christeller, J. T., Gray, D., Gontero, B., Villeneuve, P., & Carrière, F. (2020). The digestion of galactolipids and its ubiquitous function in Nature for the uptake of the essential α-linolenic acid. *Food & Function*. https://doi.org/10.1039/D0FO01040E

Sahaka, M., Mateos-Diaz, E., Amara, S., Wattanakul, J., Gray, D., Lafont, D., Gontero, B., Launay, H., & Carrière, F. (2023). In situ monitoring of galactolipid digestion by infrared spectroscopy in both model micelles and spinach chloroplasts. *Chemistry and Physics of Lipids*, *252*, 105291. https://doi.org/10.1016/j.chemphyslip.2023.105291

Saini, R. K., & Keum, Y.-S. (2018). Omega-3 and omega-6 polyunsaturated fatty acids : Dietary sources, metabolism, and significance — A review. *Life Sciences*, *203*, 255-267. https://doi.org/10.1016/j.lfs.2018.04.049

Sarkis, J., & Vié, V. (2020). Biomimetic Models to Investigate Membrane Biophysics Affecting Lipid–Protein Interaction. *Frontiers in Bioengineering and Biotechnology*, *8*. https://www.frontiersin.org/articles/10.3389/fbioe.2020.00270

Sias, B., Ferrato, F., Grandval, P., Lafont, D., Boullanger, P., De Caro, A., Leboeuf, B., Verger, R., & Carrière, F. (2004). Human Pancreatic Lipase-Related Protein 2 Is a Galactolipase. *Biochemistry*, *43*(31), 10138-10148. https://doi.org/10.1021/bi049818d

Verger, R., Mieras, M. C. E., & Haas, G. H. de. (1973). Action of Phospholipase A at Interfaces. *Journal of Biological Chemistry*, *248*(11), 4023-4034.

Wattanakul, J., Sahaka, M., Amara, S., Mansor, S., Gontero, B., Carrière, F., & Gray, D. (2019). In vitro digestion of galactolipids from chloroplast-rich fraction (CRF) of postharvest, pea vine field residue (haulm) and spinach leaves. *Food & Function*, *10*(12), 7806-7817. https://doi.org/10.1039/C9FO01867K

Wieloch, T., Borgström, B., Piéroni, G., Pattus, F., & Verger, R. (1982). Product activation of pancreatic lipase. Lipolytic enzymes as probes for lipid/water interfaces. *Journal of Biological Chemistry*, *257*(19), 11523-11528. https://doi.org/10.1016/S0021-9258(18)33792-X

Withers-Martinez, C., Carrière, F., Verger, R., Bourgeois, D., & Cambillau, C. (1996). A pancreatic lipase with a phospholipase A1 activity : Crystal structure of a chimeric pancreatic lipase-related protein 2 from guinea pig. *Structure*, *4*(11), 1363-1374. https://doi.org/10.1016/S0969-2126(96)00143-8

Xu, L., & Zuo, Y. Y. (2018). Reversible Phase Transitions in the Phospholipid Monolayer. *Langmuir*, *34*(29), 8694-8700. https://doi.org/10.1021/acs.langmuir.8b01544

FIGURES

Figure captions.

Figure 1 – 5×5 µm² AFM images of A) GL, B) GL/DPPC/pS, and C) MGDG/DGDG/SQDG/PG monolayers at 20 mN/m.

Figure 2 – A) Kinetic evolution of surface pressure (π, mN/m, red circles) and ellipsometric angle (Δ, °, blue triangle) upon the adsorption and kinetic activity of gPLRP2 (0.128 mg/L) onto GL monolayer. B) AFM images of Langmuir-Blodgett samples after 1) 35 minutes and 2) 1 hour kinetic of gPLRP2 adsorption onto GL monolayer, respectively.

Figure 3 – Schematic representation of galactolipid lipolysis by PLRP2. MGDG – monogalactosyldiacylglycerol, DGDG – digalactosyldiacylglycerol, FFA – Free fatty acid, MGMG – monogalactosylmonoacylglycerol, DGMG – digalactosylmonoacylglycerol, MGG – monogalactosylglycerol, DGG – digalactosylglycerol.

Figure 4 – Kinetic evolution of the surface pressure (π, mN/m, red circle) and the ellipsometric angle (Δ, °, blue triangle) over one hour after the injection of the inactive variant of gPLRP2 in the subphase of the GL monolayer. B) 5×5 µm² images of the Langmuir-Blodgett sample obtained after 1 hour kinetic.

Figure 5 – A) Kinetic evolution of surface pressure (π, mN/m, red circles) and ellipsometric angle (Δ, °, blue triangle) upon the adsorption and kinetic activity of gPLRP2 (0.128 mg/L) onto GL/DPPC/pS monolayer. B) AFM images of Langmuir-Blodgett samples after 1) 45 minutes and 2) 1h45 kinetic of gPLRP2 adsorption onto GL/DPPC/pS monolayer, respectively.

Figure 6 – A) Evolution of the surface pressure (π, red, mN/m) and the ellipsometric angle (Δ, blue, °) upon the adsorption of gPLRP2 onto MGDG/DGDG/SQDG/PG (1h kinetic). B) AFM images (5×5 µm²) of the interface of MGDG/DGDG/SQDG/PG (1h kinetic, π=8.5 mN/m, Δ=5.2°).

Figure 7 – Typical evolution of the particle diameter distribution of A) GL, and B) GL/DPPC/pS dispersed diluted liposomes (0.04%) in the absence and presence (4 mM NaTDC) of bile salts. Results were obtained by DLS measurements.

Figure 8 – AFM images (5×5 µm²) of substrates and lipolysis products obtained at T5min and deposited at 7.2 ± 0.1 mN/m at the air/water interface of A) GL, and B) GL/DPPC/pS monolayers. For each identified domain, the mean height level was given in the table and was obtained as an average over three sections of the image. Lipophilic substrates and products were extracted using Folch method.

Figure 1

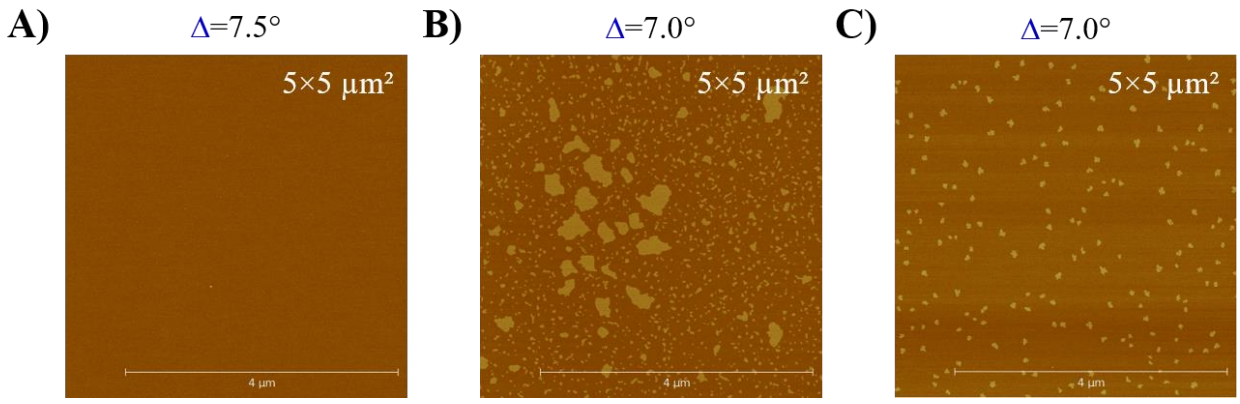

Figure 2

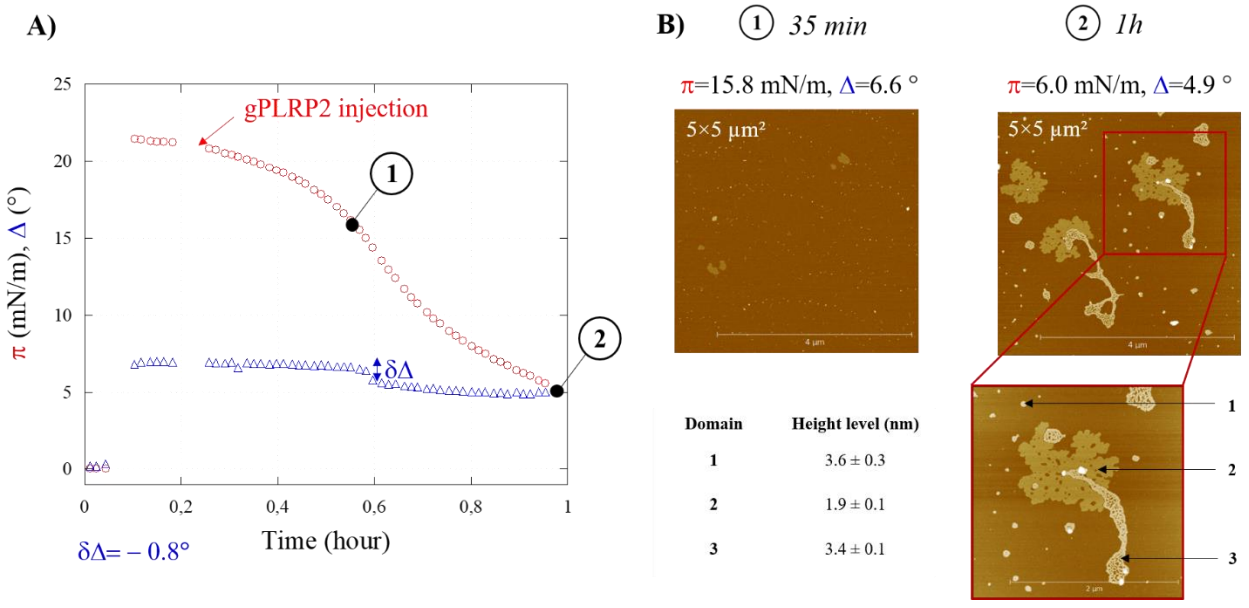

841 **Figure 3**

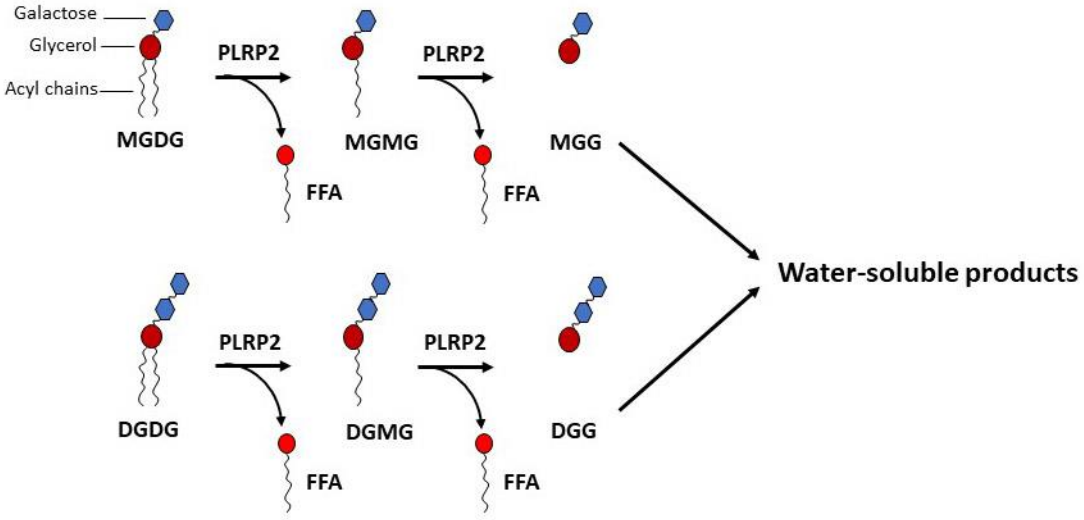

842

843 **Figure 4**

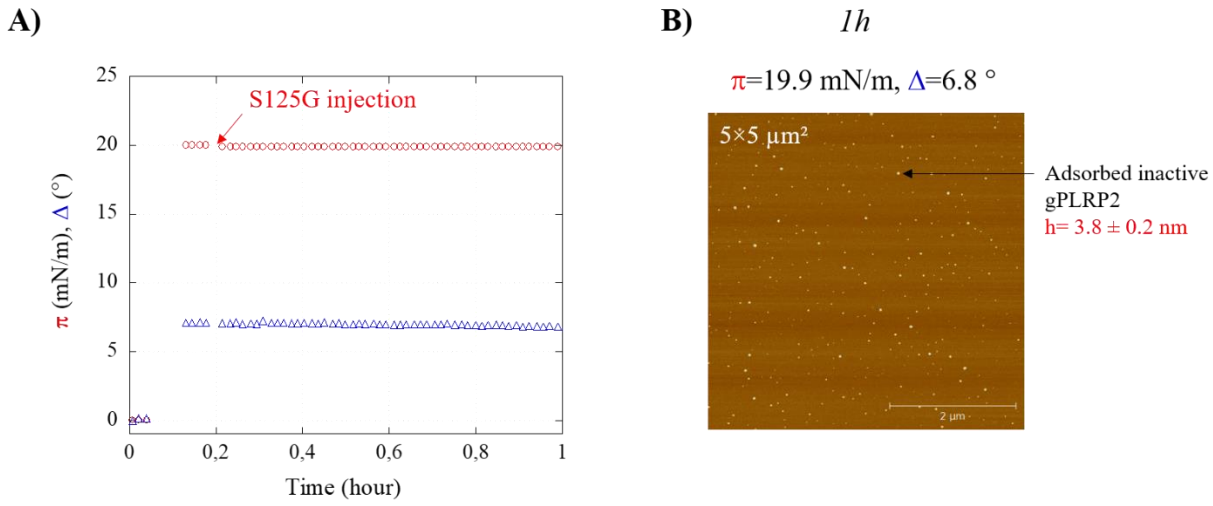

844

845

Figure 5

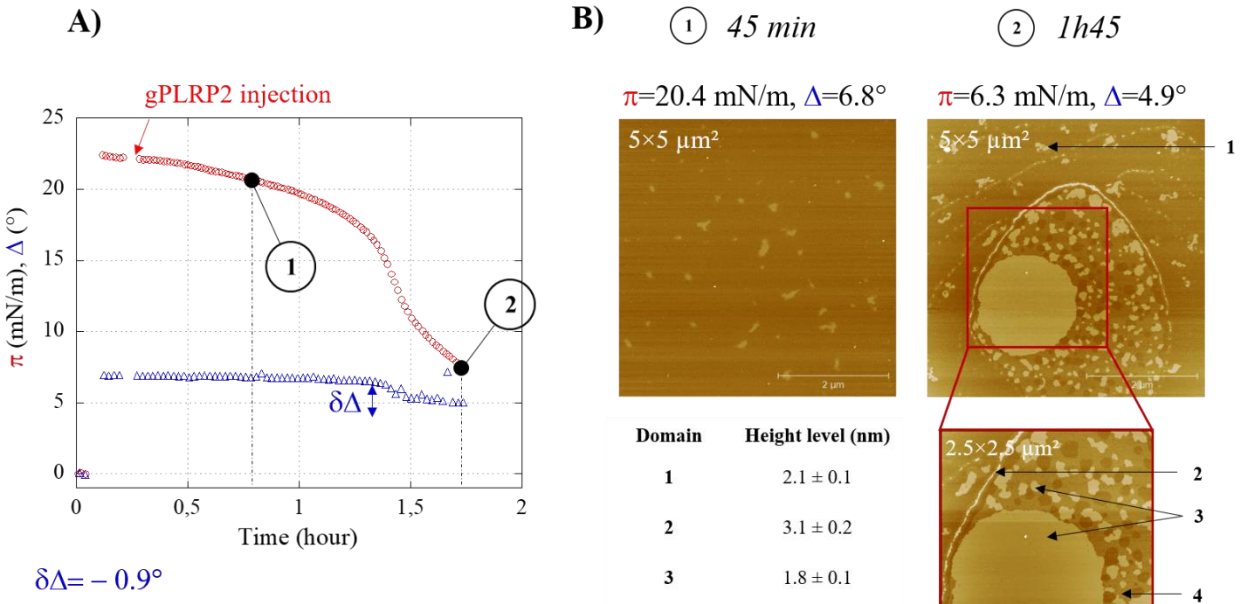

Figure 6

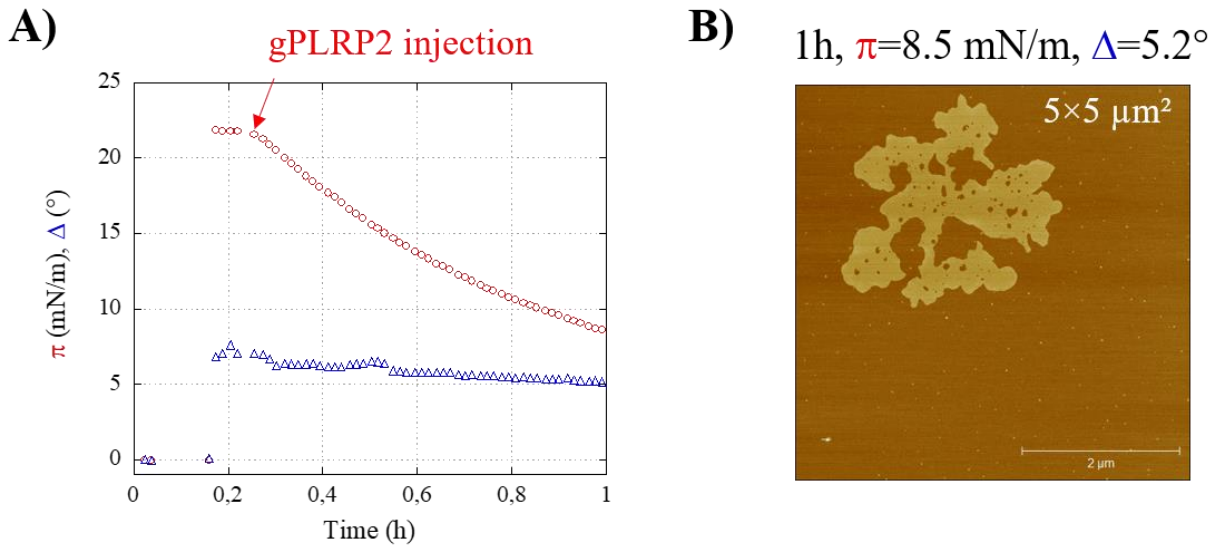

Figure 7

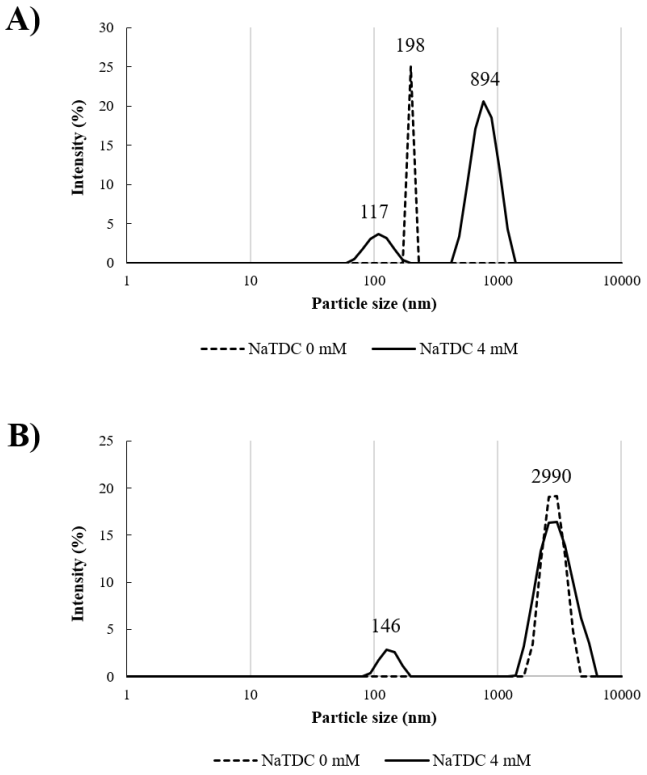

Figure 8

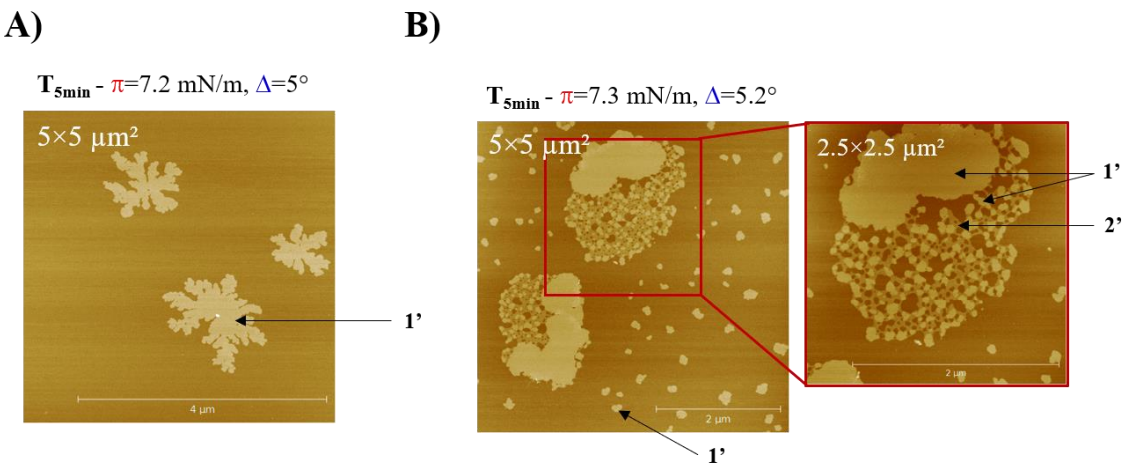

Domain	Height level (nm)
T_{5min} - 1'	1.9 ± 0.1

Domain		Height level (nm)
T_{5min}	1'	1.7 ± 0.1
	2'	1.2 ± 0.2

TABLES

Table 1 – Quantitative determination of lipid classes composition obtained by TLC at T_0 and after 5 minutes (T_{5min}) digestion by gPLRP2 of GL/DPPC/pS, GL, MGDG/DGDG/SQDG/PG liposomes. The reaction was performed at pH 7 in Tris HCl buffer containing 4 mM of NaTDC. Data are given in relative percentages of the total lipids.

	GL/DPPC/pS		**GL**		**MGDG/DGDG/SQDG/PG**	
Relative %	T_0	T_{5min}	T_0	T_{5min}	T_0	T_{5min}
FFA	7.2 ± 1.1	31.1 ± 4.5	-	43.8 ±7.5	-	54.3 ± 2.4
MGDG	40.3 ± 0.5	10.3 ± 3.0	48.2 ± 0.3	4.9 ± 1.5	65.4 ± 1.0	10.6 ± 0.1
MGMG	0.3 ± 0.1	20.0 ± 1.3	-	18.8 ± 2.2	-	31.3 ± 2.2
DGDG	33.9 ± 0.9	15.2 ± 0.6	51.8 ± 0.3	3.1 ± 0.8	34.6 ± 1.0	3.7 ± 0.1
DGMG	3.5 ± 2.7	3.8 ± 0.9	-	29.5 ± 3.5	*n.q.*	*n.q.*
DPPC	7.3 ± 3.7	10.1 ± 1.0	-	-	-	-
Lyso-PC	-	2.9 ± 1.6			-	-
pS	7.5 ± 0.7	6.4 ± 0.3	-	-	-	-
SQDG	-	-	-	-	24.7 ± 0.4	2.3 ± 0.3

**n.q. – non-quantifiable*

862 **Supplementary Material**

863 **Table S1 -** Molar composition of mixed Langmuir monolayers used as model membranes

	Monolayer composition
(1) GL	MGDG/DGDG 60:40 mol.mol^{-1}
(2) GL/DPPC	MGDG/DGDG/DPPC 30:20:50 mol.mol^{-1}.mol^{-1}
(3) GL/DPPC/pS	MGDG/DGDG/DPPC/pS* 27:18:45:10 mol.mol^{-1}1.mol^{-1}.mol^{-1}

β-sitosterol, campesterol, brassicasterol 50:40:10 mol.mol^{-1}.mol^{-1}

864

865 **Figure S2 –** Fatty acid distribution of MGDG and DGDG purchased from Avanti Polar Lipids

866

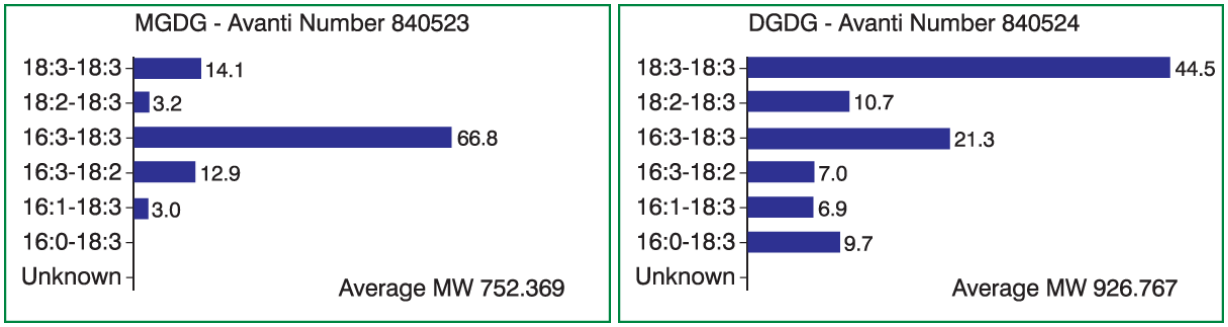

867

868

869 **Figure S3 –** Lipid classes composition obtained by TLC after 1h45 digestion by gPLRP2 of
870 GL/DPPC/pS monolayer, showing the appearance of FFA at the interface. The reaction was
871 performed at pH 7 in Tris HCl buffer in the absence of NaTDC.

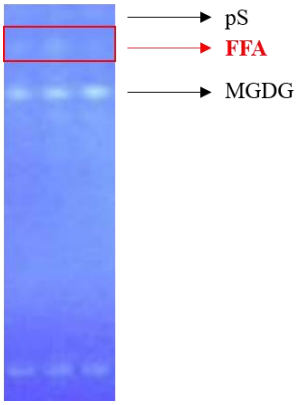

Table S4 - Quantitative determination of lipid classes composition obtained by TLC at T_0 and after 5 minutes (T_{5min}) digestion by gPLRP2 of GL/DPPC/pS liposomes **in absence of NaTDC**. The reaction was performed at pH 7 in Tris HCl buffer. Data are given in relative percentages of the total lipids.

	GL/DPPC/pS	
Relative %	T_0	T_{5min}
FFA	9.2 ± 3.1	4.9 ± 0.5
MGDG	41.2 ± 2.9	42.0 ± 1.0
MGMG	1.0 ± 1.4	0.5 ± 0.3
DGDG	35.8 ± 1.7	38.3 ± 2.3
DGMG	3.0 ± 0.5	4.9 ± 0.9
DPPC	2.0 ± 0.5	2.8 ± 0.4
LysoPC	-	-
pS	7.7 ± 0.6	6.5 ± 2.1

**n.q. – non-quantifiable*